# Fluorescent Single Walled Carbon Nanotube/Silica Composite Materials

B. C. Satishkumar,[†] Stephen K. Doorn,[‡] Gary A. Baker,[§] and Andrew M. Dattelbaum[†,*]

[†]Center for Integrated Nanotechnologies, Los Alamos National Laboratory, MS K771, Los Alamos, New Mexico 87545, [‡]Chemistry Division, Los Alamos National Laboratory, MS J563, Los Alamos, New Mexico 87545, and [§]Chemical Sciences Division, Oak Ridge National Laboratory, Oak Ridge, Tennessee 37831

**ABSTRACT** We present a new approach for the preparation of single walled carbon nanotube silica composite materials that retain the intrinsic fluorescence characteristics of the encapsulated nanotubes. Incorporation of isolated nanotubes into optically transparent matrices, such as sol−gel prepared silica, to take advantage of their near-infrared emission properties for applications like sensing has been a challenging task. In general, the alcohol solvents and acidic conditions required for typical sol−gel preparations disrupt the nanotube/surfactant assembly and cause the isolated nanotubes to aggregate leading to degradation of their fluorescence properties. To overcome these issues, we have used a sugar alcohol modified silica precursor molecule, diglycerylsilane, for encapsulation of nanotubes in silica under aqueous conditions and at neutral pH. The silica/nanotube composite materials have been prepared as monoliths, at least 5 mm thick, or as films (<1 mm) and were characterized using fluorescence and Raman spectroscopy. In the present work we have investigated the fluorescence characteristics of the silica encapsulated carbon nanotubes by means of redox doping studies as well as demonstrated their potential for biosensing applications. Such nanotube/silica composite systems may allow for new sensing and imaging applications that are not currently achievable.

**KEYWORDS:** carbon nanotubes · fluorescence · sol−gel · silica · sensing · DGS · NIR

Single walled carbon nanotubes (SWNTs) possess unique mechanical, electrical and optical properties due to their nanoscale structure based on cylindrical graphene sheets.[1] Several researchers have taken advantage of these properties to make new composite materials with improved characteristics.[2] To date, most of the new materials containing SWNTs encapsulated in a matrix of, for example, polymer or silica have been developed to utilize the intrinsic mechanical toughness[3] or high thermal conductivity of SWNTs.[4] Utilizing the optical response from SWNTs, however, is currently more challenging,[5−7] because synthesis procedures for nanotubes form both fluorescent semiconducting tubes, as well as nonfluorescent metallic nanotubes, which act to quench the emission signal from the semiconducting tubes.[8,9] Although efficient methods to separate the two fractions are under development,[10−14] their unique advantages for optical and electrical applications are still being investigated. Routine isolation of nanotubes in solution can currently be accomplished through interaction with surfactant molecules.[8,9] The resulting isolated SWNT/surfactant assembly is known to emit light in the near-infrared (NIR) region, which has prompted their application in a variety of *in vitro* and *in vivo* sensing and imaging studies.[15,16] Further, researchers have used the optical signal from semiconducting nanotubes to study redox interactions of SWNTs with solubilized dye and transition metal complexes to elucidate a number of chirality selective reaction trends that may have important implications for sensors, electronic applications, and separations of SWNTs.[17,18] For example, reversible fluorescence quenching studies have been reported for sensing biomolecular species in solution media with high selectivity and sensitivity.[18,19] Thus, incorporation of fluorescent SWNTs into a supporting matrix can allow one to make new materials that are potentially useful for sensing studies, as well as for a host of other applications.[20−22]

Silica is an ideal material for encapsulation of fluorescent materials, as it is generally inert, optically transparent, and permeable. In addition, silica can be prepared from molecular precursors in solution through sol−gel processes that can take advantage of fluorescent SWNTs dispersed in aqueous solutions. However, traditional sol−gel procedures[23] occur in alcohol solvents at acidic pH conditions. Such environmental conditions cause nanotube/surfactant assemblies to disassociate resulting in nanotube aggregation and, hence, loss of their fluorescence properties. To our knowledge, only a single procedure has been used to successfully prepare fluorescent SWNT/silica composite materials.[24] However, the authors of

*Address correspondence to amdattel@lanl.gov.

Received for review June 17, 2008 and accepted October 24, 2008.

**Published online November 7, 2008.** 10.1021/nn8003839 CCC: $40.75

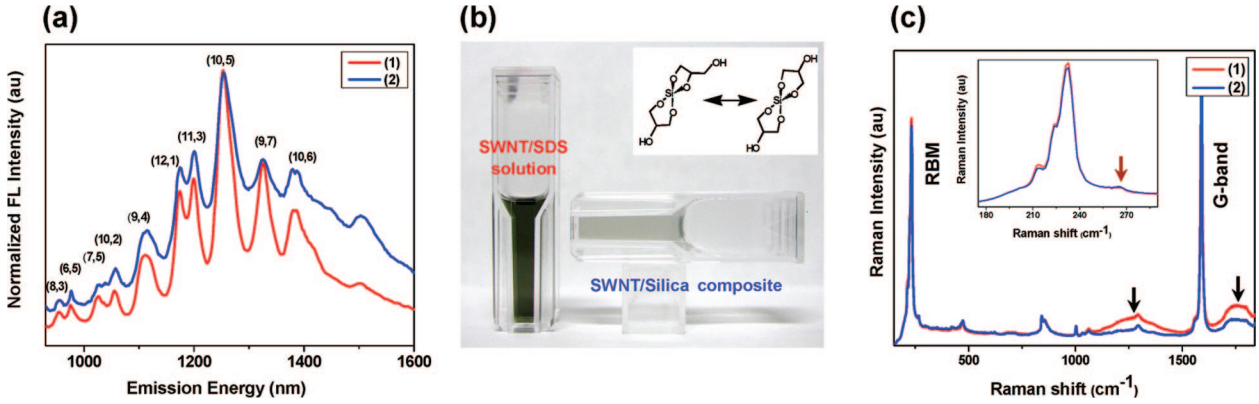


**Figure 1. (a) Normalized fluorescence spectra recorded on (1) a SWNT/SDS dispersion in $D_2O$ and (2) a SWNT/silica monolith prepared using the SWNT/SDS solution shown in (1). (b) Photograph showing a SWNT/SDS aqueous dispersion (upright cuvette) and a SWNT/silica monolith (tilted cuvette). Inset shows the possible molecular structures of the silica precursor DGS. (c) Raman spectra of (1) a SWNT/SDS dispersion in $D_2O$ and (2) a SWNT/silica monolith. Inset shows the radial breathing mode (RBM) spectra of the samples.**

this study use a multistep chemical procedure that involves the release of a toxic gas (HF) to prepare a SWNT/silica composite that loses its fluorescence as the silica film dries out. Therefore, new variations on standard sol−gel systems are needed to prepare SWNT/silica materials with stable optical signals.

Here we report the use of a sugar alcohol modified silane molecular precursor for the preparation of a silica matrix that can encapsulate fluorescently active SWNTs. Sugar alcohol modified polyol silanes have been extensively used for the encapsulation of biomolecules because these materials condense at neutral pH while releasing a benign sugar alcohol molecule.[25−27] Specifically, diglycerylsilane (DGS) was used to prepare new SWNT/silica composite materials as monoliths (thickness $>$ 5 mm) or as films (thickness $<$ 1 mm). These materials are shown by fluorescence and Raman spectroscopy to maintain the unique optical properties that originate from isolated SWNTs. Further, reversible redox-doping and emission quenching experiments were carried out on the SWNT/silica materials to illustrate their feasibility for sensing applications.

## RESULTS AND DISCUSSION

**Fluorescent SWNT/Silica Composite Materials.** We prepared SWNT/silica composite materials starting from dispersions of SWNTs in a surfactant solution that typically contained sodium dodecyl sulfate (SDS). As stated above, isolated semiconducting SWNTs in aqueous solution have a NIR emission signal, whereas aggregated mixtures of semiconducting and metallic SWNTs are not fluorescent.[8,9] The fluorescence spectrum from a SWNT/SDS dispersion in $D_2O$ is shown in Figure 1a (red spectrum) and is typical of SDS-dispersed SWNTs excited at 780 nm.[17] Multiple emission peaks are observed due to bandgap variation with chirality[9] for various nanotubes, which are noted in Figure 1a. The SWNT/SDS solution was then used to prepare SWNT/silica composite materials *via* the condensation of DGS, which was synthesized using a previously reported procedure.[28] The possible molecular structures of DGS are shown in Figure 1b (inset). The SWNT/SDS dispersion and DGS-derived SWNT/silica monolith samples were in liquid and semisolid phase, respectively, as seen in the photograph shown in Figure 1b. The cuvette on the left (upright) is a sample of a typical SWNT/SDS dispersion, while the cuvette on its side shows a SWNT/silica composite sample. Emission from SWNTs encapsulated in the DGS-derived silica (blue spectrum in Figure 1a) is similar to that of the SWNTs in solution, as most of the emission features are retained upon encapsulation. However, a red shift (∼1−3 meV) for the fluorescence features of the SWNT/silica composite relative to those in solution was observed. With the average band gap of semiconducting nanotubes being ∼1 eV, the observed red shift due to silica encapsulation is negligible. We also note that the peak fluorescence intensity for the composite sample is lower by a factor of 3 compared to a concentration-matched SWNT/SDS solution sample (although this is not obvious from the normalized emission data shown in Figure 1a). The reduction in emission intensity for the encapsulated SWNTs is most likely due to scattering losses from the silica monolith rather than from nanotube aggregation, based on Raman spectra collected on the SWNT/silica materials (see below). However, it is also possible that some interaction between the SWNTs and silica occurs to quench the fluorescence signal, as described previously.[24] Nevertheless, these data confirm that the formation of glycerol upon DGS condensation does not significantly disrupt the SWNT-surfactant assembly, that is, glycerol does not cause nanotube aggregation, in contrast to other alcohols, such as ethanol and methanol, which form during traditional sol−gel processes.

The isolated state of the nanotubes in the DGS-derived silica was further supported by Raman spectroscopy. Raman spectra, shown in Figure 1c, were taken with 785 nm excitation on SWNT/SDS assemblies in solution (red spectrum; line 1) and in a DGS-derived silica monolith (blue spectrum; line 2). In general, the spectra

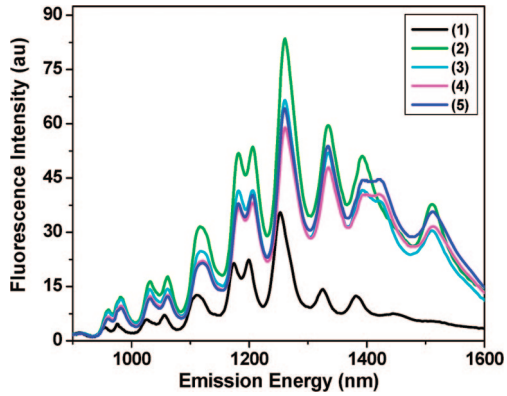


**Figure 2. Fluorescence spectra of (1) a solution of SWNT/SDS in $D_2O$ and a SWNT/SDS dispersion with the addition of (2) 1%, (3) 2%, (4) 4%, and (5) 8% P123 (w/v) in $D_2O$ at pH 7. All of the samples are concentration matched.**

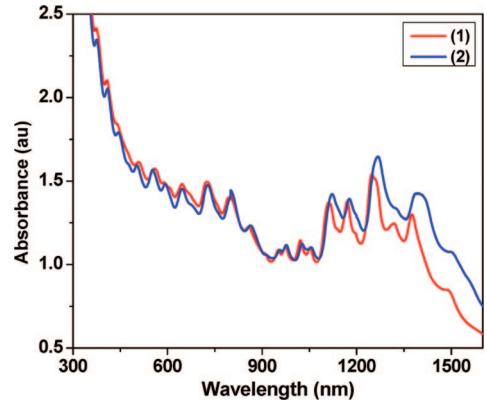


**Figure 3. UV−vis spectra of (1) SDS solubilized SWNTs and (2) SDS/P123 (1% wt/vol) solubilized SWNTs in $D_2O$ at pH 7.**

show that the observed Raman modes are identical in structure and similar in relative intensity when compared for the two samples. The similarity of the relative intensities of the RBM and G-band features as well as the appearance of broad fluorescence features in the Raman spectra for the solution and monolith samples indicate that the nanotubes are well dispersed/isolated.[29] These fluorescence bands at ~1323 $cm^{-1}$ and ~1800 $cm^{-1}$ and occurring at 876 and 914 nm absolute wavelength, respectively (see black arrows in Figure 1c) are due to emission from (6,4) and (9,1) nanotubes, respectively.[9] Note also that both spectra show a very weak Raman feature at ~267 $cm^{-1}$ (see brown arrow in the inset). It is well-known that this feature (the RBM of the (10,2) nanotube) grows in relative strength with roping of nanotubes and is routinely observed as a strong peak in as-synthesized, highly bundled, HiPco SWNT samples with Raman excitation at 785 nm.[29−31] The fact that the feature is relatively very weak in Figure 1c emphasizes the claim that isolated nanotubes are dominant in the silica composite materials prepared in the present studies. These data further illustrate the fact that the electronic structure of nanotubes is not altered upon encapsulation in DGS-derived silica, indicating negligible nanotube aggregation.

**Enhanced Fluorescence from SWNT/Surfactant Assemblies.** To enhance the fluorescence intensity of SWNTs in aqueous solutions, we added nonionic polymer surfactants, like P123, along with SDS. We note that previous reports have shown that polymeric surfactants like P123 have been used to disperse SWNTs in aqueous media,[32] but never in combination with SDS. As seen in Figure 2, the addition of P123 (1, 2, 4, and 8% w/v in $D_2O$ at pH = 7) to a SWNT/SDS dispersion resulted in enhanced fluorescence intensities relative to the starting SWNT/SDS sample (black spectrum, line 1, in Figure 2). At concentrations >8% w/v of P123, the SWNT began to precipitate into aqueous solution. We also found that upon addition of P123 to a SWNT/SDS aqueous dispersion no change in pH was observed, as determined by a pH meter. Further, consistent with previous work,[32] the nanotube fluorescence features shift slightly to the red (~5−10 meV) over the entire chirality range upon interaction with P123 (see Figure 2). Most notable, however, is that the peak fluorescence intensity for these solution mixtures is almost twice that of the starting dispersion in SDS (concentration of nanotubes was the same in all samples). The intensity enhancements are observed over the entire spectral range, indicating that most of the SWNT chiralities are affected by addition of P123. We do, however, see a significant relative enhancement in the fluorescence features at longer wavelength (at ~1423 and ~1510 nm) in the presence of P123. The fluorescence enhancement may be due to wrapping of the polymer around the nanotubes in a homogeneous fashion, which further isolates the nanotubes. Alternatively, and perhaps more likely, the observed fluorescence enhancement may be attributed to a reduction in the number of protons associated with the SWNTs. Protonation has recently been shown to cause hole-doping in solubilized nanotubes, leading to a reduction of SWNT emission efficiency.[33,34] Removal of hole-doping has been accomplished with the addition of base to SWNT solutions, which resulted in an increase in several visible absorption bands.[33] UV−vis data, shown in Figure 3, taken on a SWNT/SDS solution at pH 7 before and after addition of P123, show a significant enhancement within the $E_{11}$ transition manifold (1100−1600 nm), which is consistent with previously published results observed upon a reduction of proton-SWNT interactions.[33,34] We also collected fluorescence and UV−vis data on different aqueous SWNT/SDS/P123 samples under basic conditions (pH = 10; see Supporting Information, Figure S1). No significant increases in absorption or emission were observed by either spectroscopic technique at the higher pH. This is in contrast to SWNT/SDS dispersions that show increases in both absorption and emission upon increase in pH from 7 to 10 (see Supporting Information, Figure S2). Further, direct comparison of SWNT/SDS samples at pH 10 with SWNT/SDS/P123 (1 wt %) samples (concentration matched) show very little intensity differences

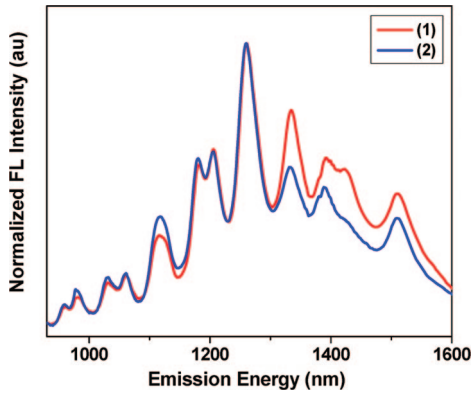


**Figure 4. Fluorescence spectra (normalized) of (1) a SWNT/SDS dispersion combined with P123 (1% w/v) at pH 7 and (2) a SWNT/silica monolith prepared from a SWNT/SDS/P123 solution.**

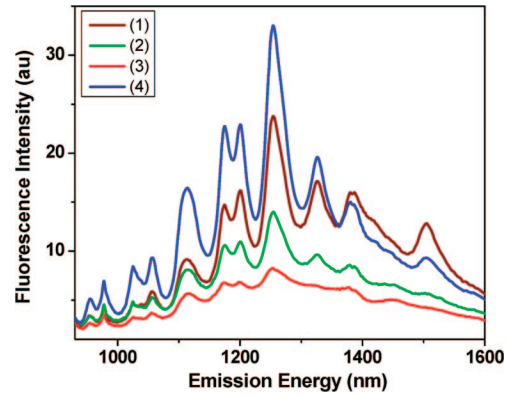


**Figure 5. Fluorescence spectra showing the reversible nature of the AB doping process. (1) Fluorescence spectrum from the initial SWNT/silica sample, and AB bleached spectra after (2) $t = 4$ min and (3) $t = 10$ min following the doping process. (4) Fluorescence spectrum from a doped sample after the addition of NADH.**

between the spectra and only a slight red shift in emission for P123 samples (see Supporting Information, Figure S2). Thus, addition of P123 appears to chemically alter the SWNT/SDS dispersion resulting in increased absorption and emission signals in a similar manner to that observed from addition of base to SWNT/SDS solutions.

SWNT/silica composites were then prepared as described above, except using a SWNT/SDS/P123 dispersion. The emission data shown in Figure 4 were collected on a SWNT/SDS/P123 (1% w/v) solution (red spectrum, line 1) as well as on a SWNT/silica monolith (blue spectrum, line 2). Once again the emission features for the nanotubes remain intact and are very slightly red-shifted upon encapsulation in silica. We also note that the emission from the solution dispersions containing P123 were more intense than a similar concentration of only SWNT/SDS encapsulated in silica. Further, in all cases studied, SWNT/silica samples stored in capped cuvettes were found to have minimal bundling over time, as determined by the observation of their fluorescence signal for at least 6 months (see Supporting Information, Figure S3). This behavior is in contrast to SWNT/SDS dispersions in solution that can show aggregation over similar periods of time. Thus, the silica gel matrix appears to help the nanotubes remain in an isolated and stable state.

**Reactivity Studies on Encapsulated SWNTs.** Although the SWNTs were encapsulated in silica, their fluorescence signals could be attenuated by exposure to small organic dopant molecules. It is known that anionic surfactants like SDS are small enough to be sterically mobile on the SWNT surface and allow access to organic dopant molecules in solution.[17] As reported previously, small aromatic molecules, like 4-amino-1,1-azobenzene-3,4-disulphonic acid (AB), accept electrons from SWNTs, thus bleaching the nanotube fluorescence signal.[17] Therefore, for doping experiments on silica encapsulated SWNTs we added AB to the monoliths and then collected fluorescence spectra as a function of AB diffusion time as shown in Figure 5. Following the doping process induced by AB, we observed the bleaching (green and red spectra in Figure 5) of fluorescence features for nanotubes in the silica matrix (see the brown spectrum for emission from starting nanotubes inside the matrix). For SWNT/silica samples made from nanotubes dispersed in SDS, the doping effect shows bleaching for both the large and small diameter nanotubes (see red spectrum in Figure 5). This behavior is different than the diameter dependent quenching observed earlier for solution dispersions,[17] which could be due to matrix induced steric constraints on the dopant molecules.

We note that the peak intensity shown in Figure 5 drops to 50% of the starting value within ~2.5 min after addition of the AB. This is in contrast to the much more rapid kinetic response observed for AB quenching of fluorescence in aqueous solution (on the order of tens of seconds, depending on nanotube diameter).[17] This expected decrease in quenching rate within the monolith is likely due to AB diffusion through the silica matrix. One could minimize this limitation by working with thin films of SWNT/Silica for redox quenching and sensing studies.

We also attempted to perform similar redox quenching experiments on SWNT/Silica samples with nanotubes dispersed in SDS and P123; however, far slower bleaching of the nanotube fluorescence was observed for these composites. It was previously noted that SWNTs dispersed in PEO-PPO-PEO block copolymers required ~10× more dopant to observe bleaching effects similar to SWNT/SDS dispersions.[17] This observation may be attributed to almost complete wrapping of SWNTs by P123, which prevents close interactions between dopant molecules and the nanotubes, or a competing interaction between the block copolymer and the dopant. A similar ability to control reactant access to the nanotube surface through engineering of surfactant structure has been recently reported.[35] An alterna-

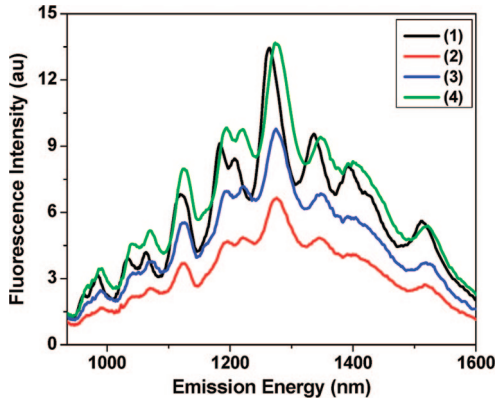


**Figure 6. Biosensing studies using SWNT/silica monoliths. Fluorescence spectra of (1) a SWNT/silica monolith and (2) after quenching by BTNA. (3) and (4) are spectra after 3 and 7 min, respectively, exposure of a BTNA quenched sample to avidin.**

tive explanation, that the dopant, AB, forms a more stable complex with the SWNT/SDS assembly,[36] does not appear likely in this case, as SDS is also present with P123, although it may be partially screened by the P123 block copolymer.

The AB bleaching effect may also be reversed chemically by adding an electron donor such as β-nicotinamide adenine dinucleotide (NADH) resulting in the complete recovery of the fluorescence spectrum (see blue spectrum in Figure 5). We note that the recovered fluorescence peak intensities for the various nanotube chiralities are greater than those for the starting sample (brown spectrum, Figure 5). This effect has been previously attributed to the reversal of doping induced by dissolved oxygen in aqueous media.[17,34−37] It is known that dissolved oxygen in water quenches the emission from large diameter semiconducting nanotubes.[34,37] In the current studies, NADH, a reducing agent, reverses the intrinsic doping induced on nanotubes by AB and dissolved oxygen, and hence, the recovered fluorescence intensities are higher than in the starting sample.

In the above studies, small molecules were used to both bleach and recover the fluorescence from encapsulated SWNTs. In subsequent studies, we made use of a small molecule, biotinylated anthracene (BTNA), as the quencher and a large protein, avidin, to recover the fluorescence signal for silica encapsulated nanotubes. This approach has been shown to be successful for biosensing studies using solubilized nanotubes.[19] Extending this approach to SWNT/silica monoliths can be advantageous as silica affords engineerable substrates. As shown in Figure 6, the initial fluorescence signal from a SWNT/silica monolith (black spectrum, line 1) is quenched upon exposure to BTNA (red spectrum, line 2). Avidin, which has a strong affinity for the biotin component of the quencher molecule, was then added and allowed to diffuse into the composite material. Fluorescence recovery data were collected for 15 min; however, almost complete recovery of the fluorescence signal was observed after 7 min (green spectrum, line 4, in Figure 6). In this case, the avidin−biotin binding leads to disruption of the quencher-nanotube interaction and hence fluorescence recovery is observed. It is noteworthy that the large avidin molecules (molecular weight ~ 66000 Daltons) are able to diffuse through the silica matrix and bind with quencher molecules lying close to the nanotube surface. These experiments open the possibility of performing biosensing studies using the SWNT/silica composites, although diffusion of biomolecules larger than avidin may limit the platform's future applicability.

**Reactivity Studies on SWNT/Silica Films.** For many device applications, it may be highly desirable to have composite materials formed into films, which decreases the diffusion path-length through the sample, potentially resulting in faster response times, as well as decreasing the amount of the analyte molecule needed for sensing. Therefore, SWNT/silica composite films (thickness <1 mm) were prepared and utilized for further redox-doping studies. A weak fluorescence spectrum could be observed from films following 2−3 days of aging (see Supporting Information, Figure S4). In addition, Raman measurements on the thin film samples of SWNT/silica showed similar features as monolith samples (see Supporting Information, Figure S5). Again, the fluorescence features in the Raman spectra from SWNT/SDS/P123 films were more intense than in SWNT/SDS films.

Redox doping experiments with AB were carried out on SWNT/SDS/silica films and monitored by Raman spectroscopy in this case (Figure 7a). The effect of AB-induced bleaching on the radial breathing mode in the Raman spectrum for SWNT encapsulated in DGS-derived silica films occurs in a manner similar to doping experiments in solution monitored by fluorescence response.[17] As shown in Figure 7, the radial breathing mode features gradually decrease in intensity after exposure to AB. Much less AB (~1/10) was needed to bleach the Raman signal from the SWNTs encapsulated in the thin films compared to SWNTs encapsulated in monolith samples, which indicates that the films may be better architectures for future sensing device applications.

Storage of the thin films for longer time (~3 months) in air caused the films to dry out and crack. We note that the dried SWNT/silica thin films show a somewhat more intense Raman feature at ~267 $cm^{-1}$ (Figure 7b, line 1), indicating some degree of increased aggregation relative to monoliths or fresh thin film samples. However, the dried films maintain Raman spectra showing a RBM intensity pattern that still represents good nanotube dispersion, that is, the RBM features (due primarily to the (12,1), (11,3), (10,5), and (9,7) chiralities) between 200 and 250 $cm^{-1}$ still dominate the spectrum. Furthermore, intensity within this family of chiralities shows a steady decrease as chiral angle increases, as

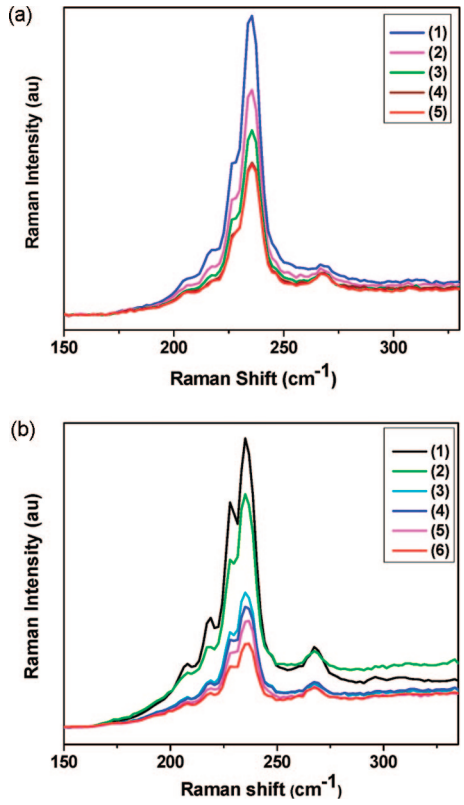


**Figure 7. Redox doping by AB of Raman features for SWNTs encapsulated in silica thin films that were (a) freshly prepared and (b) dried for ~3 months in air. (a) (1) RBM of the initial SWNT/silica film (freshly prepared film), (2)−(5) show spectra after 20, 40, 60, and 80 s, respectively, of AB doping. (b) (1) RBM of the SWNT/silica film (aged for 3 months), (2)−(6) show spectra after 1, 2, 3, 4, and 7 min, respectively, of AB doping.**

seen for the spectra of the original dispersions as well (see Figure 7a and 1c for example). Upon aggregation, the intensity pattern is expected to shift so that the "roping peak" at 267 $cm^{-1}$ dominates and the smooth progression in intensity of the (12,1) through (9,7) features would be disrupted,[29,30] which is not observed in this case. We also note that the weak (6,4) and (9,1) fluorescence bands are still present in the dried film Raman spectra, serving as a further indicator that rebundling has not occurred to any significant extent in the dried film (data not shown). While such highly deteriorated films would be considered suboptimal from an applications standpoint, these results serve to further highlight the robustness of such films in terms of their ability to stabilize against nanotube aggregation. In fact, the dried films remain suitable for performing redox doping studies as illustrated in Figure 7b.

## CONCLUSIONS

We have developed a new approach for the preparation of SWNT/silica composite materials that are fluorescently active. This approach makes use of diglyceryl silane, a sugar alcohol based silica precursor molecule, which condenses under conditions that do not promote significant aggregation of the surfactant-nanotube assemblies, as illustrated by fluorescence and Raman spectroscopy. Reversible redox doping experiments on SWNT/silica monoliths and films demonstrate that the SWNTs are accessible to both small redox agents and fairly large proteins even though the SWNTs remain encapsulated within the silica. This work shows that these nanocomposite materials may be potentially useful for more complex biosensing studies in the future. As the current approach for silica based composite materials offers engineerable monoliths or thin film substrates, it has a unique potential for applications involving biosensing. For example, because the synthesis of DGS-derived silica is a biocompatible process, one can consider encapsulating and stabilizing nanotube-protein assemblies, like the SWNT-hydrogenase materials recently reported, for energy related applications.[38] Furthermore, because negligible bundling of nanotubes is observed over several months, one may attempt to align nanotubes within DGS-derived silica using mechanical techniques or magnetic fields to prepare composite materials with interesting optical and mechanical properties. Experimental efforts in these areas are currently underway.

## METHODS

**Preparation of SWNT Dispersions.** Surfactant isolated SWNT dispersions were prepared from SWNTs synthesized by high-pressure decomposition of carbon monoxide (HiPco).[8,17] The nanotubes (~40 mg SWNTs in 180 mL water) were shear mixed with 1 wt % sodium dodecylsulphate (SDS) in $D_2O$ (or $H_2O$), followed by ultrasonication and centrifugation at 140000 × g for 4 h. This procedure yielded an aqueous dispersion of individualized nanotubes functionalized by SDS molecules. Various nonionic polymer surfactants, such as pluronics 123 ($PEO_{20}$-$PPO_{70}$-$PEO_{20}$), were also added to the SWNT/SDS dispersions. Aqueous nonionic polymer surfactants at various w/v % were added to SWNT/SDS suspensions in a 1:1 volume ratio by mixing at room temperature for 10−12 h. pH measurements on SWNT/surfactant samples were made using a pH meter.

Fluorescence spectra were recorded using a NIR fluorimeter based on a Thermo Nicolet NXR 9600 FTIR paired with a Ge detector (a 780 nm diode laser was used as the excitation source). Raman measurements were performed using a laser operating at 785 nm with a liquid nitrogen cooled CCD array using a single grating monochromator. The laser power at the sample was 10−15 mW and Raman spectra were integrated over 10 s.

**Synthesis of SWNT/Silica Composite Materials.** The SWNT/SDS dispersions in $D_2O$ were used to prepare SWNT/Silica composite materials *via* the condensation of DGS [$Si(C_3H_6O_3)_2$], which was synthesized following a previously reported procedure[28] and then lyophilized for 4 days. In a typical silica monolith preparation ~150 mg of DGS was partially dissolved in ~500 μL SDS (aq; 1% SDS w/v) in a bath sonicator at 10−15 °C for 30 min. The resulting solution was filtered through a 1.0 μm polycarbonate filter to remove any undissolved particulates of DGS and then mixed in a plastic cuvette with ~500 μL of a SWNT/SDS dispersion. The capped samples were allowed to gel at ~4 °C for 48 h, yielding SWNT/silica monoliths. SWNT/silica composite films (thickness <1 mm) were prepared by pipetting ~200 μL of the SWNT/SDS/DGS or SWNT/SDS/P123/DGS solution into cover

wells (1 mm deep, Grace BioLabs), then allowed to gel at 4 °C for at least 3 days.

**Redox Doping and Sensing Studies on SWNT/Silica Materials.** For doping experiments on SWNT/silica monoliths, we used an aromatic molecule, 4-amino-1,1-azobenzene-3,4-disulphonic acid (AB, Aldrich). We added ~30 μL of AB (0.1 M (aq)) to the monoliths and then monitored the fluorescence spectra as a function of AB diffusion time. In a similar manner, we used AB (10 μL, 0.05 M (aq)) to induce bleaching of the radial breathing mode in the Raman spectrum for SWNTs encapsulated in DGS-derived silica thin films. For SWNT/SDS solution studies, 15 μL of 0.1 M AB (aq) was added to ~1 mL of a SWNT solution to study redox doping.

SWNT/silica monoliths were used for sensing of proteins such as avidin. In these studies, we made use of a conjugated dye complex, biotinylated anthracene (BTNA, synthesized according to ref 19), to induce quenching of nanotube fluorescence. Later, avidin (10 μL, 0.03 mM (aq)), which has a strong affinity for the biotin component of the quencher molecule, was added and allowed to diffuse into the composite material. This resulted in the recovery of the quenched fluorescence for nanotubes encapsulated in the silica matrix.

*Acknowledgment.* The authors would like to thank H.-L. Wang for the biotinylated-anthracene and the Department of Energy, Basic Energy Sciences, for providing funding for this work.

*Supporting Information Available:* Fluorescence and Raman spectroscopic data on SWNTs in DGS-derived silica films, as well as UV−vis and fluorescence data on SWNT/SDS solutions with and without additional P123 at pH 7 and 10, are available free of charge *via* the Internet at http://pubs.acs.org.

## REFERENCES AND NOTES

1. Rotkin, S. V.; Subramoney, S. *Applied physics of carbon nanotubes: Fundamentals of theory, optics and transport devices*; Springer: New York, NY, 2005.
2. Xie, X-L.; Mai, Y-W.; Zhou, X-P. Dispersion and Alignment of Carbon Nanotubes in Polymer Matrix: A Review. *Mater. Sci. Eng.* **2005**, *R49*, 89–112.
3. Schadler, L. S.; Giannaris, S. C.; Ajayan, P. M. Load Transfer in Carbon Nanotube Epoxy Composites. *Appl. Phys. Lett.* **1998**, *73*, 3842–3844.
4. Biercuk, M. J.; Llaguno, M. C.; Radosavljevic, M.; Hyun, J. K.; Johnson, A. T.; Fischer, J. E. Carbon Nanotube Composites for Thermal Management. *Appl. Phys. Lett.* **2002**, *80*, 2767–2769.
5. Kim, Y.; Minami, N.; Kazaoui, S. Highly Polarized Absorption and Photoluminescence of Stretch-Aligned Single-Wall Carbon Nanotubes Dispersed in Gelatin Films. *Appl. Phys. Lett.* **2005**, *86*, 073103-1–073103-3.
6. Graff, R. A.; Swanson, J. P.; Barone, P. W.; Baik, S.; Heller, D. A.; Strano, M. S. Achieving Individual-Nanotube Dispersion at High Loading in Single-Walled Carbon Nanotube Composites. *Adv. Mater.* **2005**, *17*, 980–984.
7. Fagan, J. A.; Simpson, J. R.; Landi, B. J.; Richter, L. J.; Mandelbaum, I.; Bajpai, V.; Ho, D. L.; Raffaelle, R.; Hight Walker, A. R.; Bauer, B. J.; et al. Dielectric Response of Aligned Semiconducting Single-Wall Nanotubes. *Phys. Rev. Lett.* **2007**, *98*, 147402-1–147402-4.
8. O'Connell, M. J.; Bachilo, S. M.; Huffman, C. B.; Moore, C. M.; Strano, M. S.; Haroz, E. H.; Rialon, K.; Boul, P. J.; Noon, W. H.; Kittrell, C.; et al. Band Gap Fluorescence from Individual Single-Walled Carbon Nanotubes. *Science* **2002**, *297*, 593–596.
9. Bachilo, S. M.; Strano, M. S.; Kittrell, C.; Hauge, R. H.; Smalley, R. E.; Weisman, R. B. Structure-Assigned Optical Spectra of Single-Walled Carbon Nanotubes. *Science* **2002**, *298*, 2361–2366.
10. Yang, C.; Park, J. S.; An, K. H.; Lim, S. C.; Seo, K.; Kim, B.; Park, K. A.; Han, S.; Chong Yun Park, C. Y.; Lee, Y. H. Selective Removal of Metallic Single-Walled Carbon Nanotubes with Small Diameters by Using Nitric and Sulfuric Acids. *J. Phys. Chem. B* **2005**, *109*, 19242–19248.
11. Krupke, R.; Hennrich, F.; Lohneysen, H. V.; Kappes, M. M. Separation of Metallic from Semiconducting Single-Walled Carbon Nanotubes. *Science* **2003**, *301*, 344–347.
12. Kim, S. N.; Luo, Z.; Papadimitrakopoulos, F. Diameter and Metallicity Dependent Redox Influences on the Separation of Single-Wall Carbon Nanotubes. *Nano Lett.* **2005**, *5*, 2500–2504.
13. Miyata, S.; Maniwa, Y.; Kataura, H. Selective Oxidation of Semiconducting Single-Wall Carbon Nanotubes by Hydrogen Peroxide. *J. Phys. Chem. B* **2006**, *110*, 25–29.
14. Arnold, M. S.; Green, A. A.; Hulvat, J. F.; Stupp, S. I.; Hersam, M. C. Sorting Carbon Nanotubes by Electronic Structure Using Density Differentiation. *Nat. Nanotechnol.* **2006**, *1*, 60–65.
15. Cherukuri, P.; Bachilo, S. M.; Litovsky, S. H.; Weisman, R. B. Near-Infrared Fluorescence Microscopy of Single-Walled Carbon Nanotubes in Phagocytic Cells. *J. Am. Chem. Soc.* **2004**, *126*, 15638–15639.
16. Cherukuri, P.; Gannon, C. J.; Leeuw, T. K.; Schmidt, H. K.; Smalley, R. E.; Curley, S. A.; Weisman, R. B. Mammalian Pharmacokinetics of Carbon Nanotubes Using Intrinsic Near-Infrared Fluorescence. *Proc. Natl. Acad. Sci. U.S.A.* **2006**, *103*, 18882–18886.
17. O'Connell, M. J.; Eibergen, E. E.; Doorn, S. K. Chiral Selectivity in the Charge-Transfer Bleaching of Single-Walled Carbon Nanotube Spectra. *Nat. Mater.* **2005**, *4*, 412–418.
18. Barone, P. W.; Baik, S.; Heller, D. A.; Strano, M. S. Near-Infrared Optical Sensors Based on Single-Walled Carbon Nanotubes. *Nat. Mater.* **2005**, *4*, 86–92.
19. Satishkumar, B. C.; Brown, L. O.; Gao, Y.; Wang, C. C.; Wang, H. L.; Doorn, S. K. Reversible Fluorescence Quenching in Carbon Nanotubes for Biomolecular Sensing. *Nat. Nanotechnol.* **2007**, *2*, 560–564.
20. Zhang, M.; Fang, S.; Zakhidov, A. A.; Lee, S. B.; Aliev, A. E.; Williams, C. D.; Atkinson, K. R.; Baughman, R. H. Strong, Transparent, Multifunctional Carbon Nanotube Sheets. *Science* **2005**, *309*, 1215–1219.
21. Dellago, C.; Naor, M. M.; Hummer, G. Proton Transport through Water-Filled Carbon Nanotubes. *Phys. Rev. Lett.* **2003**, *90*, 105902−1105902−4.
22. Yang, Z. P.; Ci, L.; Bur, J. A.; Lin, S. Y.; Ajayan, P. M. Experimental Observation of an Extremely Dark Material Made By a Low-Density Nanotube Array. *Nano Lett.* **2008**, *8*, 446–451.
23. Brinker, C. J.; Scherer, G. W. *Sol-Gel Science: The Physics and Chemistry of Sol-Gel. Processing*; Academic Press: New York, 1990.
24. Whitsitt, E. A.; Moore, V. C.; Smalley, R. E.; Barron, A. R. LPD Silica Coating of Individual Single Walled Carbon Nanotubes. *J. Mater. Chem.* **2005**, *15*, 4678–4687.
25. Besanger, T. R.; Chen, Y.; Deisingh, A. K.; Hodgson, R.; Jin, W.; Mayer, S.; Brook, M. A.; Brennan, J. D. Screening of Inhibitors Using Enzymes Entrapped in Sol-Gel-Derived Materials. *Anal. Chem.* **2003**, *75*, 2382–2391.
26. Gadre, S. Y.; Gouma, P. I. Biodoped Ceramics: Synthesis, Properties, and Applications. *J. Am. Ceram. Soc.* **2006**, *89*, 2987–3002.
27. Avnir, D.; Coradin, T.; Levc, O.; Livage, J. Recent Bio-Applications of Sol-Gel Materials. *J. Mater. Chem.* **2006**, *16*, 1013–1030.
28. Brook, M. A.; Chen, Y.; Guo, K.; Zhang, Z.; Brennan, J. D. Sugar-Modified Silanes: Precursors for Silica Monoliths. *J. Mater. Chem.* **2004**, *14*, 1469–1479.
29. Doorn, S. K.; Strano, M. S.; O'Connell, M. J.; Haroz, E. H.; Rialon, K. L.; Hauge, R. H.; Smalley, R. E. Capillary Electrophoresis Separations of Bundled and Individual Carbon Nanotubes. *J. Phys. Chem. B* **2003**, *107*, 6063–6069.
30. O'Connell, M. J.; Sivaram, S.; Doorn, S. K. Near-Infrared Resonance Raman Excitation Profile Studies of Single-Walled Carbon Nanotube Intertube Interactions: A Direct Comparison of Bundled and Individually Dispersed HiPco Nanotubes. *Phys. Rev. B: Condens. Matter Mater. Phys.* **2004**, *69*, 235415-1–235415-15.

31. Heller, D. A.; Barone, P. W.; Swanson, J. P.; Mayrhofer, R. M.; Strano, M. S. Using Raman Spectroscopy to Elucidate the Aggregation State of Single-Walled Carbon Nanotubes. *J. Phys. Chem. B* **2004**, *108*, 6905–6909.
32. Moore, V. C.; Strano, M. S.; Haroz, E. H.; Hauge, R. H.; Smalley, R. E. Individually Suspended Single-Walled Carbon Nanotubes in Various Surfactants. *Nano Lett.* **2003**, *3*, 1379–1382.
33. Blackburn, J. L.; McDonald, T. J.; Metzger, W. K.; Engtrakul, C.; Rumbles, G.; Heben, M. J. Protonation Effects on the Branching Ratio in Photoexcited Single-Walled Carbon Nanotube Dispersions. *Nano Lett.* **2008**, *8*, 1047–1054.
34. Strano, M. S.; Huffman, C. B.; Moore, V. C.; O'Connell, M. J.; Haroz, E. H.; Hubbard, J.; Miller, M.; Rialon, K.; Kittrell, C.; Ramesh, S.; et al. Reversible, Band-Gap-Selective Protonation of Single-Walled Carbon Nanotubes in Solution. *J. Phys. Chem. B* **2003**, *107*, 6979–6985.
35. Duque, J. G.; Cognet, L.; Parra-Vasquez, A. N. G.; Nichols, N.; Schmidt, H. K.; Pasquali, M. Stable Luminescence from Individual Carbon Nanotubes in Acidic, Basic, and Biological Environments. *J. Am. Chem. Soc.* **2008**, *130*, 2626–2633.
36. Zheng, M.; Diner, B. A. Solution Redox Chemistry of Carbon Nanotubes. *J. Am. Chem. Soc.* **2004**, *126*, 15490–15494.
37. Dukovic, G.; White, B. E.; Zhou, Z.; Wang, F.; Jockusch, S.; Steigerwald, M. L.; Heinz, T. F.; Friesner, R. A.; Turro, N. J.; Brus, L. E. Reversible Surface Oxidation and Efficient Luminescence Quenching in Semiconductor Single-Wall Carbon Nanotubes. *J. Am. Chem. Soc.* **2004**, *126*, 15269–15276.
38. McDonald, T. J.; Svedruzic, D.; Kim, Y. H.; Blackburn, J. L.; Zhang, S. B.; King, P. W.; Heben, M. J. Wiring-Up Hydrogenase with Single-Walled Carbon Nanotubes. *Nano Lett.* **2007**, *7*, 3528–3534.